Mechanism of Phosphatidylinositol-Specific Phospholipase C: A Unified View of the Mechanism of Catalysis[†,‡]

Robert J. Hondal,[§] Zhong Zhao,[§] Alexander V. Kravchuk,[§] Hua Liao,[||] Suzette R. Riddle,[||] Xiangjun Yue,[⊥] Karol S. Bruzik,*[,⊥] and Ming-Daw Tsai*[,§,||,▽]

Departments of Chemistry and Biochemistry and Ohio State Biochemistry Program, The Ohio State University, Columbus, Ohio 43210, and Department of Medicinal Chemistry and Pharmacognosy, College of Pharmacy, University of Illinois at Chicago, Chicago, Illinois 60612

Received October 24, 1997

ABSTRACT: The mechanism of phosphatidylinositol-specific phospholipase C (PI-PLC) has been suggested to resemble that of ribonuclease A. The goal of this work is to rigorously evaluate the mechanism of PI-PLC from *Bacillus thuringiensis* by examining the functional and structural roles of His-32 and His-82, along with the two nearby residues Asp-274 and Asp-33 (which form a hydrogen bond with His-32 and His-82, respectively), using site-directed mutagenesis. In all, twelve mutants were constructed, which, except D274E, showed little structural perturbation on the basis of 1D NMR and 2D NOESY analyses. The H32A, H32N, H32Q, H82A, H82N, H82Q, H82D, and D274A mutants showed a 10^4-10^5-fold decrease in specific activity toward phosphatidylinositol; the D274N, D33A, and D33N mutants retained 0.1−1% activity, whereas the D274E mutant retained 13% activity. Steady-state kinetic analysis of mutants using (2*R*)-1,2-dipalmitoyloxypropane-3-(thiophospho-1D-*myo*-inositol) (DPsPI) as a substrate generally agreed well with the specific activity toward phosphatidylinositol. The results suggest a mechanism in which His-32 functions as a general base to abstract the proton from 2-OH and facilitates the attack of the deprotonated 2-oxygen on the phosphorus atom. This general base function is augmented by the carboxylate group of Asp-274 which forms a diad with His-32. The H82A and D33A mutants showed an unusually high activity with substrates featuring low pK_a leaving groups, such as DPsPI and *p*-nitrophenyl inositol phosphate (NPIPs). These results suggest that His-82 functions as the general acid with assistance from Asp-33, facilitating the departure of the leaving group by protonation of the glycerol O3 oxygen. The Brønsted coefficients obtained for the WT and the D33N mutant indicate a high degree of proton transfer to the leaving group and further underscore the "helper" function of Asp-33. The complete mechanism also includes activation of the phosphate group toward nucleophilic attack by a hydrogen bond between Arg-69 and a nonbridging oxygen atom. The overall mechanism can be described as "complex" general acid−general base since three elements are required for efficient catalysis.

Phosphatidylinositol-specific phospholipase C (PI-PLC)[1] plays a key role in receptor-mediated transformations of inositol phospholipids (*1*−*4*). The products of mammalian PI-PLC play important biological roles because they serve as a source of intracellular signaling molecules, diacylglycerol and inositol 1,4,5-trisphosphate. Diacylglycerol activates protein kinase C (*5*), and inositol 1,4,5-trisphosphate is involved in releasing intracellular calcium stores (*6*). The released calcium then activates many types of cellular processes. Glycosylphosphatidylinositol-specific phospholipase C, a subclass of PI-PLC, cleaves the spacer arm of glycosylphosphatidylinositol-anchored proteins to release extracellular enzymatic activities of these proteins (*7*).

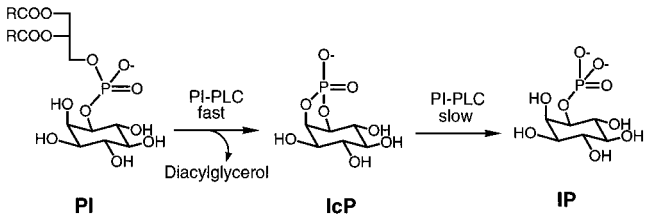

FIGURE 1: Conversion of phosphatidylinositol to IcP and IP catalyzed by *B. thuringiensis* PI-PLC.

As shown in Figure 1, the reaction of bacterial PI-PLC consists of two steps: fast cleavage of PI into lipid-soluble diacylglycerol and water-soluble *myo*-inositol 1,2-cyclic phosphate (IcP), and slow hydrolysis of IcP to *myo*-inositol 1-phosphate (IP). Conversion of PI to IcP is 100−1000-fold faster than hydrolysis of IcP to IP depending on the conditions used (*8*, *9*). On the basis of the stereochemical course of the reaction and the X-ray structure of PI-PLC complex with *myo*-inositol, a mechanism involving general base−general acid catalysis, reminiscent of that of ribonuclease A, has been proposed for both steps (*8*, *10*−*13*) as

[†] This work was supported by NIH Grant GM 30327. The DMX-600 NMR spectrometer used was funded in part by NIH Grant RR08299 and NSF Grant BIR-9221639.

[‡] Part of the results described in this paper has been presented in the Third FASEB Summer Conference on Phospholipases, July 22−27, 1995, Vermont Academy, Saxtons River, VT. This is paper 4 in the series "Mechanism of Phosphatidylinositol-Specific Phospholipase C". For paper 3, see ref *19*.

* Corresponding authors.

[§] Department of Chemistry, The Ohio State University.

[||] Ohio State Biochemistry Program.

[⊥] University of Illinois at Chicago.

[▽] Department of Biochemistry, The Ohio State University.

S0006-2960(97)02646-9 CCC: $15.00
Published on Web 03/11/1998

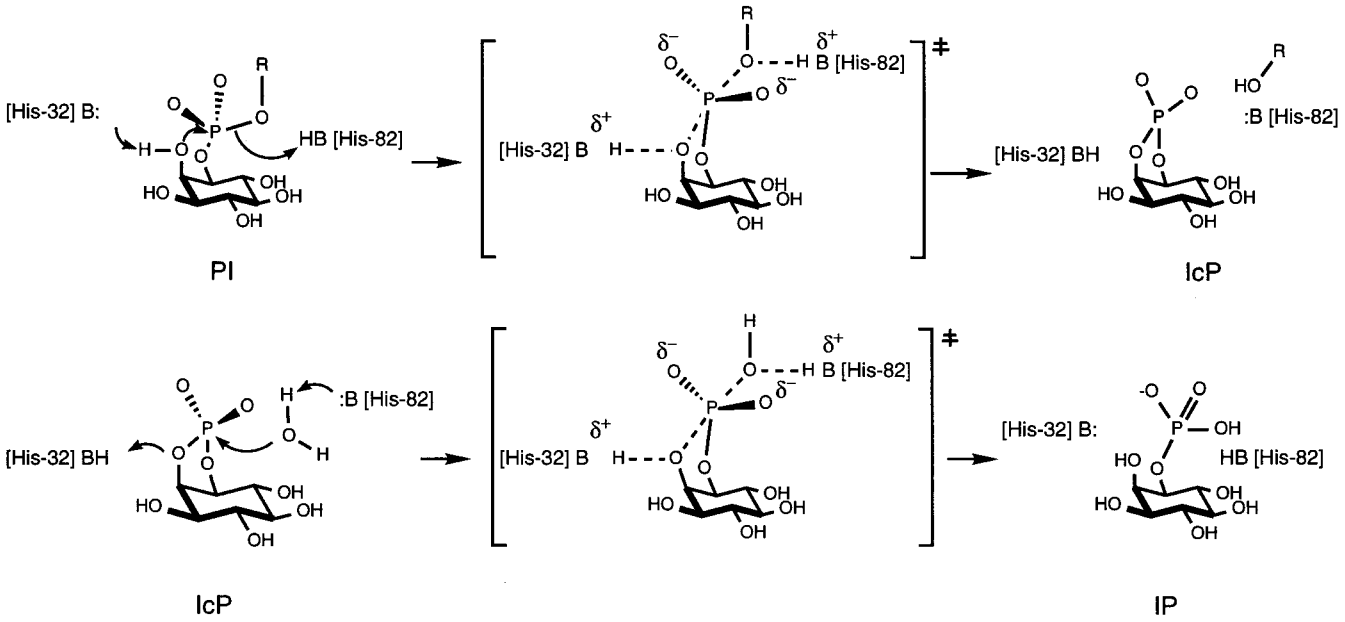

FIGURE 2: Mechanism of general acid−general base catalysis proposed on the basis of the crystal structure *(11).*

shown in Figure 2. According to the proposed mechanism, His-32 abstracts the 2-OH proton and His-82 donates a proton to the leaving group O3 oxygen of diacylglycerol in the first step (PI to IcP). The roles of His-32 and His-82 are reversed in the second step (IcP to IP): His-82 serves as a general base to activate the water molecule, whereas His-32 serves as a general acid to protonate the inositol O2 oxygen and thereby facilitate the ring opening. The general base−general acid functions of His-32 and His-82 in this mechanism are highly analogous to those of His-12 and His-119 of ribonuclease A. More recently, a crystal structure of the complex of mammalian PI-PLC-δ_1 with IP_3 and Ca^{2+} was reported, and a mechanism similar to that of the bacterial PI-PLC was proposed based on the structure (*14*, *15*). It was proposed that Ca^{2+} acted to lower the pK_a of the 2-OH group of inositol or to stabilize the highly negatively charged transition state. The bacterial PI-PLCs are metal-independent, and this represents a difference in the catalytic mechanisms of the mammalian and bacterial enzymes.

Our studies focus on the bacterial PI-PLC from *Bacillus thuringiensis*, which has a relatively small size (35 kDa), making analyses of structure−function relationships simpler. It differs from *Bacillus cereus* PI-PLC by only eight nonconserved residues (*16*). Our recent site-directed mutagenesis studies of this enzyme coupled with NMR and stereochemical analyses demonstrated that Arg-69 interacts with the phosphate moiety of the substrate PI (*17*) and that Asp-33 is involved in facilitation of the leaving group departure (*18*, *19*). This work focuses on the two active site histidines, His-32 and His-82, and two aspartate residues, Asp-274 and Asp-33. These residues form two His−Asp pairs (Asp-33···His-82 and Asp-274···His-32, respectively) reminiscent of the catalytic diads of phospholipase A_2 (*20*) and serine proteases (*21*). All four residues are highly conserved in bacterial PI-PLCs (*16*, *22*). We have constructed twelve mutants at these four positions and examined them for potential structural perturbations by both 1D proton NMR and 2D NOESY NMR. The conformational stability of the mutants was determined by guanidine hydrochloride (Gdn-HCl) induced denaturation and circular dichroism (CD) spectroscopy. Kinetic properties of all mutants were characterized using [^{3}H]PI, the phosphorothiolate analogue of PI, and *p*-nitrophenyl inositol phosphorothioate (NPIPs) as assay substrates (*17*). To assess the function of Asp-274 and Asp-33, we have examined the pK_as of the histidine residues in WT, D274N, and D33N mutants and determined Brønsted coefficients for WT and D33N. This work allows evaluation of the four active site residues and offers new insights into the mechanism of the bacterial PI-PLC catalysis.

MATERIALS AND METHODS

Materials. Phosphatidylinositol (PI) from bovine brain and 1,2-diheptanoyl-*sn*-glycero-3-phosphocholine (DHPC) were purchased from Avanti Polar Lipids. L-α-[*myo*-inositol-2-^{3}H]Phosphatidylinositol (^{3}H-PI) was purchased from Dupont NEN. 5,5′-Dithiobis[2-nitrobenzoic acid] (DTNB) and *O*-methyl phosphorodichloridite were purchased from Aldrich. Enantiomerically pure (2*R*)-1,2-dipalmitoyloxypropane-3-(thiophospho-1D-*myo*-inositol) (DPsPI) and 2,3,4,5,6-penta-(methoxymethylene)-1D-*myo*-inositol (Figure 3, **1**) were synthesized analogously as described recently (*23*). Oligonucleotides were purchased from Integrated DNA Technologies. The pHN1403 vector was a generous gift from Frederick Dahlquist. The pMY31 was a generous gift from

[1] Abbreviations: 1D, one-dimensional; 2D, two-dimensional; CD, circular dichroism; CpA, cytidine adenosine 3′,5′-phosphate, DHPC, 1,2-diheptanoyl-*sn*-glycero-3-phosphocholine; DPsPI, 1,2-dipalmitoyloxypropane-3-(thiophospho-1D-*myo*-inositol); dsDNA, double-stranded DNA; DTNB, 5,5′-dithiobis[2-nitrobenzoic acid]; GA, general acid; GB, general base; Gdn-HCl, guanidine hydrochloride; GroPI, *sn*-glycero-3-phospho-1D-*myo*-inositol; HEPES, *N*-(2-hydroxyethyl)piperazine-*N*′-2-ethanesulfonic acid; ^{3}H-PI, L-α-[*myo*-inositol-2-^{3}H]phosphatidylinositol; IcP, inositol 1,2-cyclic phosphate; IP, inositol 1-phosphate; IP_3, D-*myo*-inositol 1,4,5-trisphosphate; kDa, kilodalton; MOPS, 4-morpholinepropanesulfonic acid; NMR, nuclear magnetic resonance; NOESY, nuclear Overhauser enhancement spectroscopy; PI, phosphatidylinositol; PI-PLC, phosphatidylinositol-specific phospholipase C; ssDNA, single-stranded DNA; TMP, trimethyl phosphate; TMSP-d_4, sodium 3-(trimethylsilyl)propionate-*2*,*2*,*3*,*3*-d_4; Tris, 2-amino-2-(hydroxymethyl)-1,3-propanediol; UpC, uridine cytidine 3′,5′-phosphate; cUMP, uridine 2′,3′-cyclic phosphate; WT, wild type.

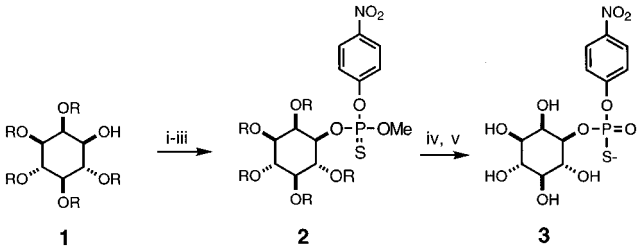

FIGURE 3: Synthesis of diastereomers of *p*-nitrophenyl inositol phosphate (NPIPs). *R*, methoxymethylene; i, Cl_2P-OMe, iPr_2EtN; ii, *p*-nitrophenol, iPr_2EtN; iii, S_8; iv, Me_3N; v, $EtSH/BF_3$-Et_2O.

Johannes Volwerk. The *Escherichia coli* strain MM294 was obtained from New England Biolabs. The *E. coli* strains CJ236 and JM101 used for mutagenesis were purchased from Stratagene. All DNA-modifying enzymes were from New England Biolabs, and Taq DyeDeoxy terminator cycle sequencing kits were from Applied Biosystems. Ultrapure guanidine hydrochloride was purchased from ICN Biochemicals. TMSP-d_4, 99.9% atom D D_2O, and "100%" D_2O were purchased from Cambridge Isotope Laboratories. All other reagents were of the highest quality available commercially.

Construction and Purification of Mutant Enzymes. The site-directed mutants presented here were generated by the method of Kunkel (*24*). The PI-PLC gene with the STII signal sequence (obtained from pMY31) was subcloned into RF M13mp19 using the restriction sites *Xba*I and *Sph*I. A single-stranded uracil DNA template of M13mp19-PLC was prepared by transfecting *E. coli* CJ236 cells. Oligonucleotides used for constructing H32A, H32N, H32Q, D274A, D274N, and D274E were 5′-TCCAGGAACAGCTGATAGTGGGA, 5′-CCAGGAACAAACGATAGT, 5′-AGGAACACAGGATAGTGGG, 5′-TGGGTAATTCAAGCTTACATAAATGAAAAG, 5′-GGGTAATTCAAAACTACATAAATG, and 5′-GTAATTCAAGAATACATAAATG, respectively, where the underlined bases represent the mutation site. The oligonucleotides 5′-CGATAGTTCTTCATGCTGGGCCATTATATC, 5′-CGATAGTTCTTCATAACGGGC−CATTATATC, 5′-CGATAGTTCTTCATCAGGGGCCATTATATC, 5′-CGATAGTTCT-TCATGACGGGCCATTATATC, 5′-AGGAACACACGCGAGTGGGACGT, and 5′-CC-AGGAACACACAATTCCGGGACGTTCAAG were used for constructing H82A, H82N, H82Q, H82D, D33A, and D33N mutants, respectively. After mutagenesis reactions, ssDNAs of M13mp19-PIPLC were isolated and screened by sequencing. DyeDeoxy terminator cycle sequencing kits were used, and the sequencing was carried out on a Applied Biosystems model 373A DNA sequencer. The mutant genes were then subcloned into pHN1403 expression vector, which contains a *lac-tac-tac* promoter, using *Xba*I and *Sph*I restriction sites. The resulting mutants were finally verified by sequencing dsDNA of the entire PI-PLC gene. PI-PLC mutants were expressed by transforming the *E. coli* cell strain MM294. Routinely, 10 L of LB was used to grow the cells (*17*). The H32A, H32N, H32Q, H82A, H82N, H82Q, and H82D mutant bacteria were grown at 30 °C; the D274A, D274N, and D274E mutants were grown at 20 °C; and the D33A and D33N mutants were grown at 24 °C. The mutant PI-PLCs were purified to homogeneity according to the procedure for WT enzyme (*17*), using a DEAE column (DE52, Whatman), a Sephadex G-100 column (Pharmacia), and a Phenyl Sepharose CL-4B column (Pharmacia). Typically, 35−50 mg of the enzyme was obtained from 10 L of culture.

*p-Nitrophenol Inositol Phosphorothioate (NPIPs, **3**).* The synthetic procedure is shown in Figure 3. To the mixture of 2,3,4,5,6-penta(methoxymethylene)-1D-*myo*-inositol (**1**, 100 mg, 0.25 mmol) and diisopropylethylamine (96 μL, 0.55 mmol) in dry dichloromethane (2 mL) was added *O*-methyl phosphorodichloridite (25 μL, 0.26 mmol) at −50 °C with stirring. After 8 h, a solution of *p*-nitrophenol (36 mg, 0.26 mmol) in dry methylene chloride was added to this mixture, and stirring was continued at room temperature for 4 h. Following solvent removal and addition of sulfur (40 mg), dry toluene (2 mL) was added and the resulting suspension was stirred at room temperature for another 10 h. Evaporation of the solvent followed by chromatography on silica gel using hexane−acetone (6:1, v/v) as the eluent gave the triester **2** (130 mg, 82%) as a colorless oil. ^{1}H NMR (200 MHz, $CDCl_3$) δ 3.35−3.45 (m, 15H), 3.45 (m, 2H), 3.85−3.95 (m, 4H), 4.08 (m, 1H), 4.30−4.47 (m, 2H), 4.75−4.95 (m, 10H), 7.37 (m, 2H), 8.25 (m, 2H). ^{31}P NMR ($CDCl_3$) δ 64.2 ppm. The triester **2** (130 mg, 0.2 mmol) was dissolved in dry liquid trimethylamine (1 mL) at −10 °C, and the resulting solution was stored at room temperature for 16 h. The amine was evaporated, and the residue was dissolved in dry ethanethiol (1 mL) and added with boron trifluoride etherate (30 μL). After 40 min all solvents were evaporated, and the residue was chromatographed on silica gel using chloroform−methanol−acetic acid (6:4:0.1, v/v) as the eluent to yield pure NPIPs (**3**, 54 mg, 66%) as a pale yellow solid. ^{1}H NMR (300 MHz, $CDCl_3$) δ 3.24 (t, 1H), 3.35 (dd, 1H), 3.63 (tr, 1H), 3.82 (t, 1H), 4.28 (m, 2H), 7.47 (m, 2H), 8.15 (m, 2H). ^{31}P NMR ($CDCl_3$) δ 54.8, 54.2 ppm (42:58 mixture of diastereomers). ES MS (*m*/*z*): 396 (m − H^+).

Specific Activity Analyses with [^{3}H]PI Substrate. The specific activities of mutants were measured according to the procedure reported earlier (*17*, *25*). ^{3}H-PI was mixed with the unlabeled PI from bovine brain to obtain an overall PI concentration of 10 mM and a specific activity of ca. 1.25 $\times$ 10^6 cpm/μmol. The reaction mixture contained 20 μL of this substrate solution, 20 μL of 0.8% sodium deoxycholate, and 40 μL of 0.1 M sodium borate, pH 7.5. An aliquot of 20 μL of PI-PLC was added to the reaction mixture and incubated at 37 °C for 10 min. The concentrations of WT PI-PLC and mutants used were adjusted so that 10−30% conversion of substrate to product could be observed within 10 min.

Steady-State Kinetic Analysis. Steady-state kinetic analysis was carried out with the thio-substrate analogue, DPsPI, according to the procedure reported earlier (*17*, *26*). The reaction conditions were 0.025−2.0 mM DPsPI in 50 mM MOPS buffer (pH 7.5), 5 μL of 50 mM DTNB in EtOH, and 5 μL of enzyme solution. The initial reaction velocity (V_o) was obtained by monitoring the change of absorbance at 412 nm. The initial reaction rate as a function of the substrate concentration was treated by curve-fitting of the data to the Michaelis−Menten equation using SigmaPlot (Jandel Corp.). The D274N, D274E, H82A, D33A, and D33N mutants were subjected to this steady-state kinetic analysis.

Specific Activity of PI-PLC and Mutants toward NPIPs and IcP. WT and mutant enzymes were assayed for activity toward NPIPs using ^{31}P NMR following the formation of

IcPs. The R_p and S_p diastereomers were used as a solution of a 58:42 mixture at 10 mM total concentration in 50 mM MOPS buffer at pH 7.5. The velocities are reported as micromoles per minute per milligram. In a separate assay, activity of WT PI-PLC and mutant enzymes toward IcP was measured, also using ^{31}P NMR. A typical assay mixture (0.5 mL) contained 16 mM DHPC, 5 mM IcP, 100 mM sodium borate buffer (pH 7.5), and 15% D_2O. These conditions are similar to the ones reported previously (*9*). For the WT enzyme, 1.5 μg was used in the assay, and as the mutants showed a wide range of activities, the amount of mutant enzyme was adjusted so that the observed rate was similar to that obtained with WT enzyme.

Determination of the pK_a of Active Site Histidine Residues. WT and mutant PI-PLC enzymes were expressed using a pET-PLC plasmid created for this purpose (*17*), in a synthetic rich medium without histidine. L-Histidine hydrochloride (ring-2-^{13}C, 99%, from Cambridge Isotope Laboratories) was added to a concentration of 50 mg/L at the time of induction. Labeled proteins were purified as described previously (*17*). Two-dimensional ^{1}H−^{13}C HSQC (*27, 28*) spectra of specifically labeled proteins at pH values ranging from 4 to 10 were recorded on a Bruker DMX 600 NMR spectrometer at 37 °C. Each sample contained 0.3−0.4 mM enzyme and 50 mM phosphate buffer in 90% H_2O/10% D_2O. The D274N mutant was found to be more stable in D_2O and thus was kept in 100% D_2O. Assignments of signals from His-32 and His-82 were made by comparing the spectrum of WT PI-PLC with those of the corresponding alanine mutants. Assignments of four other histidine signals were based on those of Liu et al. (*29*). The pH dependence of C_ϵH chemical shifts of each titratable histidine residue was fitted to the modified Henderson−Hasselbalch equation by the least-squares method:

$$\delta_{obs} = \delta_{AH} + (\delta_A - \delta_{AH})(10^{pH - pK_a})(1 + 10^{pH - pK_a})^{-1}$$

where δ_{AH} and δ_A are the chemical shifts in the fully protonated and deprotonated states, respectively.

Transesterification Reaction Catalyzed by PI-PLC. Short-chain alcohols with varying pK_a's were used to measure the rate of transesterification catalyzed by PI-PLC. These alcohols (pK_a in parentheses) were 2,2-difluoroethanol (13.3), choline (13.9), 2-fluoroethanol (14.2), methoxyethanol (14.8), and ethanol (15.9). The reaction mixture (0.5 mL) contained an alcohol (1.9 M), IcP (12 mM), MOPS buffer (pH 7.5, 100 mM), and trimethyl phosphate (TMP, 10 mM) as an internal standard, and the progress of the conversion was monitored by ^{31}P NMR. The reaction was performed with WT PI-PLC and the D33N mutant using 3.9 μg of WT and 197 μg of D33N enzymes, respectively. The initial velocity of the reaction, expressed as the amount of product formed per minute, was calculated from the ratio of the integrated signal intensity of the diester formed to that of TMP and extrapolated to time zero. The velocity of hydrolysis of IcP to IP was determined in the same way. ^{31}P NMR spectra were recorded on a Bruker AM-250 spectrometer at a spectral frequency of 101.25 MHz.

Structural Analysis Using 1D- and 2D-NMR. All spectra were obtained on a Bruker DMX-600 spectrometer at 37 °C. TMSP-d_4 was used as an internal chemical shift reference. PI-PLC samples were prepared as follows: PI-PLC fractions from the Phenyl Sepharose CL-4B column were pooled and precipitated with ammonium sulfate (576 g/L). After centrifugation for 1 h at 14000*g*, the pellet was dissolved in 10 mL of dialysis buffer (1 mM HEPES, pH 7.0), and the solution was first dialyzed at 4 °C for 8 h in 8 L of 1 mM HEPES, pH 7.0, and then for 8 h in 8 L of 0.1 mM HEPES, pH 7.0. The samples were then lyophilized and stored at −20 °C. The enzyme (4 mg) was dissolved in D_2O, incubated for 10 min to ensure exchange, and lyophilized. Finally, the sample was dissolved in 1 mL of "100%" D_2O, and the final pH (without isotope correction) was adjusted to 6.8 by using DCl and NaOD solutions.

Gdn-HCl-Induced Denaturation and Conformational Stability. CD spectra were recorded on a JASCO J-500C spectropolarimeter using a thermostated quartz microcell. A stock solution of 7.0 M Gdn-HCl was prepared with a buffer containing 10 mM borate and 0.1 mM EDTA, pH 7.5, and the exact concentration was determined by refractive index (*30*). The enzyme solution of ca. 2.5 mg/mL concentration was prepared in the same buffer, and the precise protein concentration was determined spectrophotometrically. Samples containing enzymes at 0.05 mg/mL concentration were prepared in the borate buffer indicated above with varying concentrations of Gdn-HCl. These samples were incubated at 19 °C for 10 min and then scanned 5 times from 230 to 210 nm. The ellipticity at 215 nm was recorded and used to determine the free energy of the unfolding, $\Delta G_d^{H_2O}$ (*31*).

RESULTS

Expression and Purification of Mutants. Mutants H32A, H32N, H32Q, H82A, H82N, H82Q, and H82D were expressed and purified according to the procedure used for WT PI-PLC (*17*). These mutants behaved very similarly to WT PI-PLC during the purification process. The D274A, D274N, and D274E mutants could not be expressed in the soluble form under the conditions used for WT PI-PLC. The expression was modified as follows: after induction, the cells were grown for 24 h at 20 °C, instead of 12 h at 30 °C. The D33A and D33N mutants were grown at 24 °C. All mutants were then purified to homogeneity using the same chromatographic sequence as that used for WT PI-PLC (*17*).

Specific Activity of Mutants with ^{3}H-PI Substrate. The activities of all mutants for the conversion of PI to IcP determined with ^{3}H-PI as a substrate (*17*) are shown in Table 1. All His-32 and His-82 mutants displayed 10^4−10^5-fold decreases in specific activity with respect to that of the WT enzyme. The activities of the Asp-274 mutants varied: D274A mutant showed a 10^4-fold decrease, the D274N mutant displayed a modest 64-fold decrease, and that of the D274E mutant was only 8-fold lower than that of WT PI-PLC. The mutants of Asp-33 behaved differently from the Asp-274 mutants in that the D33A and D33N mutants displayed similar reductions in activity (1000- and 310-fold decreases relative to WT, respectively). The large decreases in the activities of His-32 and His-82 mutants reported in this and a recent report from another laboratory (*33*) support the importance of these two residues in the catalytic mechanism of PI-PLC as suggested by the X-ray crystallographic structure (*11, 32*).

Steady-State Kinetic Analyses of Mutants. Recently, we and others have described a continuous assay for the

Table 1: Summary of Kinetic Data for WT and Mutant PI-PLC

	[^{3}H]PI		DPsPI	
enzyme	sp act.[a] (μmol min^{-1} mg^{-1})	rel act. (%)	V_{max}[b] (μmol min^{-1} mg^{-1})	$K_{m,app}$ (mM)[b]
WT[c]	1300	100	53.5	0.18
H32A	0.030	0.002	<0.0026	n.d.[d]
H32N	0.0135	0.001	<0.0028	n.d.
H32Q	0.0115	0.0009	<0.0031	n.d.
H82A	0.013	0.001	0.10	0.17
H82N	0.060	0.0046	n.d.	n.d.
H82Q	0.067	0.0052	n.d.	n.d.
H82D	0.004	0.0003	n.d.	n.d.
D274A	0.060	0.0046	<0.0028	n.d.
D274N	21.0	1.62	0.29 (0.5%)[e]	0.040
D274E	168	12.9	13.2 (23.5%)	0.11
D33A[f]	1.3	0.10	13.4 (25.0%)	0.031
D33N	4.3	0.33	0.75 (1.4%)	0.030

[a] Measured at 37 °C, 2.0 mM PI, and 0.4% sodium deoxycholate in 50 mM borate buffer, pH 7.5. [b] Measured at 25 °C, 0−2.0 mM DPsPI, and [DHPC]/[DPsPI] = 4.0 in, 50 mM MOPS buffer, pH 7.5. [c] Reference *17*. [d] n.d., not determined. [e] The numbers in parentheses indicate the V_{max} relative to WT. [f] Reference *18*.

conversion of PI to IcP using DPsPI, a thio analogue of DPPI (*17*, *23*, *26*). DPsPI differs from DPPI in that the oxygen atom at the 3-position of the diacylglycerol moiety is replaced by a sulfur atom. The release of the free thiol analogue of diacylglycerol by PI-PLC allows continuous measurement of the reaction rate by following the coupling of the thiol with DTNB (*26*, *34*). The V_{max} and K_m values obtained from steady-state kinetic analyses are more accurate compared to the specific activity obtained from the radioactivity assay described in the previous section. However, the V_{max} and K_m thus obtained should be considered only as apparent values, since the substrate exists as mixed micelles (with DHPC as a detergent).

The results of kinetic evaluation of mutants are also listed in Table 1. Only WT, D274N, D274E, H82A, D33N, and D33A could be assayed continuously, since the mutants with very low specific activity would fall below the limit of detection. For some mutants an upper limit of activity was estimated. The data in Table 1 indicate that, with the exception of the D33A and H82A mutants, the changes in mutants' V_{max} values relative to WT measured with the continuous assay paralleled those obtained with the ^{3}H-PI assay. As discussed below, both D33A and H82A displayed anomalously high activity using the DPsPI substrate.

D33A and H82A Mutants Display a "Reverse Thio-Effect". The "thio-effect", defined as the ratio of the rate of cleavage of the natural substrate to that of the substrate analogue in which an oxygen atom is replaced by a sulfur atom (k_O/k_S), has been widely used in the mechanistic studies of enzymes and ribozymes (*35*, *36*). The k_O and k_S values for WT PI-PLC with DPPI and DPsPI were 1300 and 53.5 units/mg (1 unit = 1 μmol min^{-1} mg^{-1}), respectively, giving a thio-effect of 24. The corresponding k_O and k_S values for D33A were 1.3 and 13.4 units/mg, respectively, giving a "reverse thio-effect" of 0.1. The analogous k_O and k_S values for H82A were 0.013 and 0.1, for a reverse thio-effect of 0.13 (for preliminary results, see ref *18*). On the basis of their activities toward the oxo-substrate, both D33A and H82A have several hundredfold higher activity with DPsPI than would be predicted. To the best of our knowledge, this is the first observation of the enhancement of the rate of enzymatic cleavage of a phosphate group due to sulfur substitution. The implications of this result with regard to the catalytic mechanism of PI-PLC are discussed later.

Table 2: Specific Activities of WT and Mutant Enzymes toward IcP[a]

enzyme	cyclic phosphodiesterase activity (μmol min^{-1} mg^{-1})
WT	22
H82A	n.d.[b]
H32A	n.d.
D33A	0.007
D33N	0.085
D274A	0.0003
D274N	2.16

[a] Assay conditions included 5 mM IcP, 16 mM DHPC, and 100 mM sodium borate, pH 7.5. [b] Not detectable.

Activity of WT, H82A, and D33A toward NPIPs. The water-soluble substrate, *p*-nitrophenol inositol phosphate (NPIP), has been previously used to measure the activity of PI-PLC (*37*). We have synthesized the phosphorothioate analogue of NPIP, (*R*p + *S*p)-NPIPs, to determine activities and stereoselectivities of the mutant enzymes toward the diastereomers of this highly reactive substrate analogue. On the basis of ^{31}P NMR assay, the specific activity of the WT enzyme was 12.8 units/mg, whereas the corresponding activities of D33A and H82A mutants were 3.63 and 0.78 units/mg, respectively, for the cleavage of the more reactive *R*p-isomer. These results show that the catalytic role of the residues at positions 82 and 33 is minimized in the case of the phosphodiester substrates featuring very good leaving groups, such as *p*-nitrophenol.

Activity of PI-PLC and Mutants toward IcP. As mentioned above, and as reported previously (*8*, *9*), PI-PLC also acts as a phosphodiesterase toward IcP. It is believed that the active site residues involved in the first step of the reaction (phosphotransferase activity) are also involved in the phosphodiesterase activity of PI-PLC (*11*). Because PI-PLC is activated toward IcP hydrolysis by the addition of a zwitterionic hydrophobic interface (*9*), the assays of phosphodiesterase activity of mutant enzymes were performed in the presence of 16 mM DHPC. The activation of PI-PLC by DHPC is important in view of its low phosphodiesterase activity, further curtailed by mutations at catalytically important positions. In the absence of DHPC, the activity of many mutants would simply be too low to detect. The velocities of the reactions derived from ^{31}P NMR time courses and expressed as specific activities in micromoles per minute per milligram are summarized in Table 2. The results show that most mutated residues, and His-32 and His-82 in particular, are important for both reactions catalyzed by PI-PLC.

Determination of the pK_a of Active Site Histidine Residues. The results shown in the preceding and earlier sections indicate the importance of Asp-274 to catalysis, most likely via its influence on His-32. Since mutation of the negatively charged aspartate should influence the pK_a of a nearby histidine, we determined the pK_a of several histidine residues of WT, D274N, and D33N mutant PI-PLC as described in Materials and Methods. Figure 4 shows the representative HSQC spectra of WT PI-PLC as the enzyme is being titrated from pH 4.2 to pH 7.9. The titration curves derived from

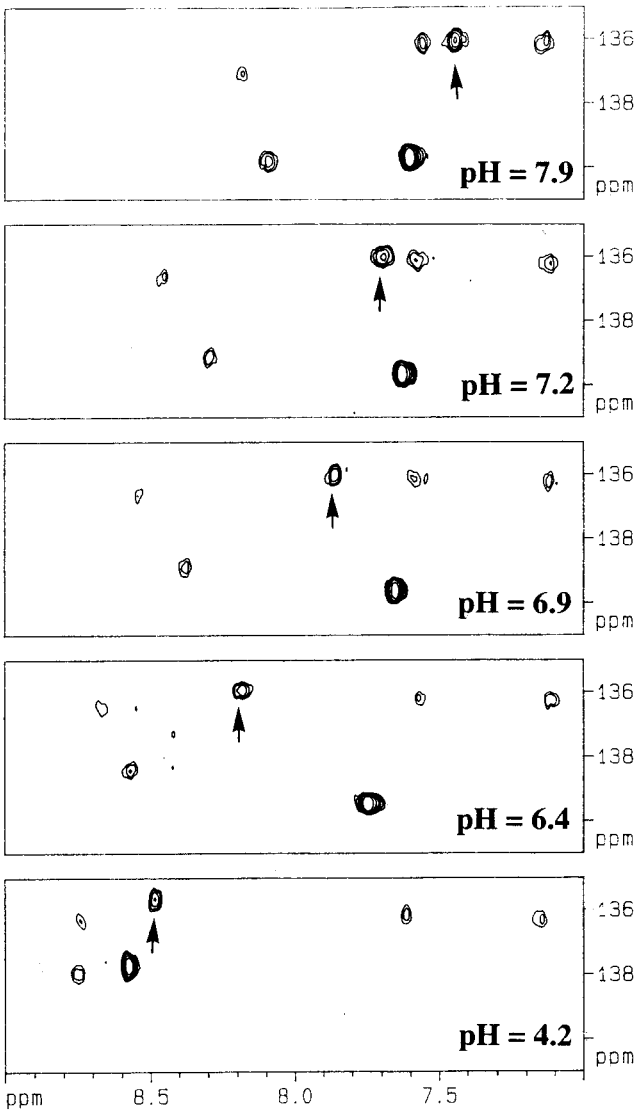

FIGURE 4: HSQC spectrum of ^{13}C-labeled histidine PI-PLC residues. The arrows show the position of the resonance belonging to His-227 as it is being titrated from pH 4.2 to 7.9.

such HSQC experiments are shown in Figure 5, and the pK_a values determined from these curves are summarized in Table 3. The results for the WT enzyme are essentially the same as those recently published for *B. cereus* PI-PLC (*29*). The greater instability of the D274N mutant prevented the unambiguous assignment of a resonance for its His-32. As a result, only the pK_a values of His-82 and His-227 were determined for this mutant, and both pK_a values in the mutant were close to those in the WT enzyme. A substantial shift in the pK_a's for His-32 and His-82 was observed in the D33N mutant (pK_a's of 0.6 and 0.8, respectively), while the pK_a's of His-92 and His-227 did not differ from those of WT PI-PLC.

Transesterification with Short-Chain Alcohols Catalyzed by PI-PLC. It has been recently shown that PI-PLC catalyzes a transesterification reaction between IcP and short-chain alcohols to yield *O*-alkyl inositol phosphates (*10*). The transesterification activity is not particularly specific with regard to alcohol structure; therefore, a series of alcohols with varying pK_a's could be used to assess the sensitivity of the reaction rate to the pK_a of the alcohol. The effect of mutation at positions 82 and 33 on the sensitivity of the rate

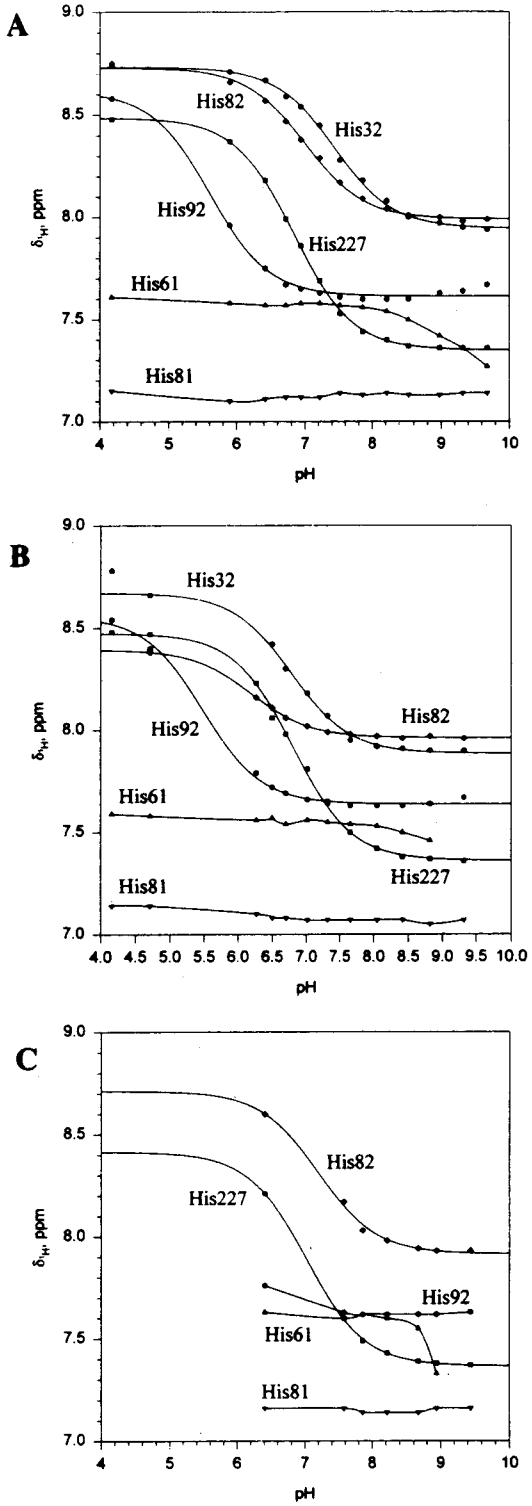

FIGURE 5: Titration curves for histidine residues of PI-PLC: (A) WT enzyme, (B) D33N mutant, and (C) D274N mutant.

of transesterification versus alcohol pK_a could also be used to provide evidence for the involvement of the His-82···Asp-33 diad in leaving group protonation. Unfortunately, the H82A mutant could not be used in transesterifications due to its very low activity; hence, the scope of this experiment was limited to WT PI-PLC and D33N mutant. The rates of transesterifications were determined for alcohols with pK_a's varying within the range of 13.3−15.9. The dependence of transesterification rate constants vs alcohol pK_a for the two enzymes is shown in panel A of Figure 6.

Table 3: pK_a Values of Titratable Histidines in WT and Mutant PI-PLC Enzymes

	His residue			
enzyme	H32	H82	H92	H227
WT	7.4	7.0	5.6	6.8
D274N	n.d.[a]	7.2	<6.5	7.0
D33N	6.8	6.2	5.5	6.8

[a] Not determined.

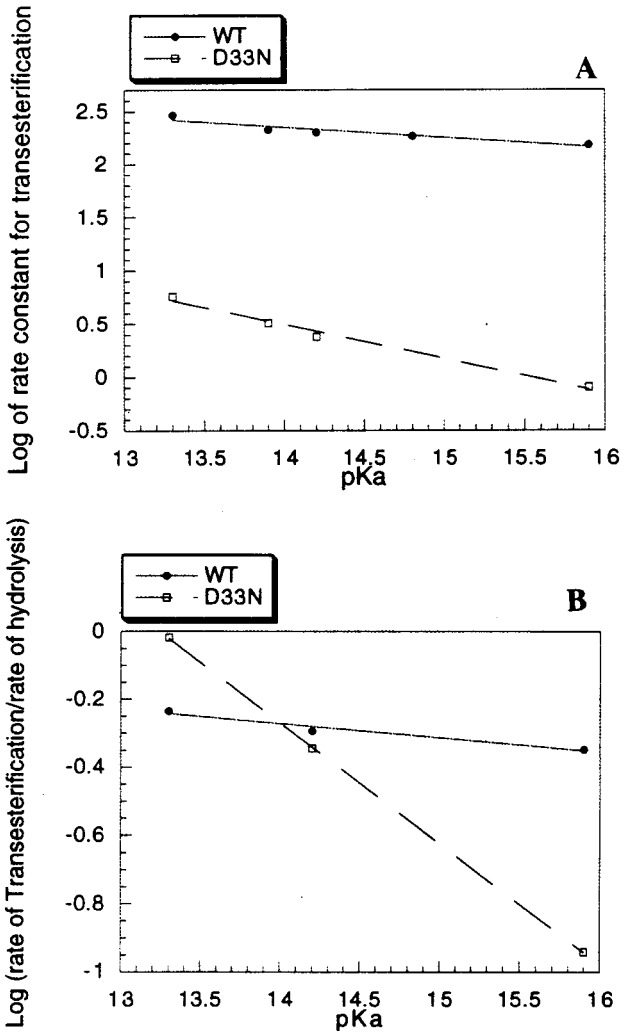

FIGURE 6: (A) Brønsted plot for the transesterification reaction catalyzed by WT PI-PLC and the D33N mutant. (B) Plot of the ratio of the rate of transesterification to the rate of hydrolysis for WT PI-PLC and the D33N mutant. The assay was performed using an alcohol (1.9 M) and IcP (12 mM) in MOPS buffer, pH 7.5, and the rates of the conversion were determined by ^{31}P NMR. The reactions were started by adding WT PI-PLC (3.9 μg) or the D33N mutant (197 μg) to the assay mixture.

These results can be summarized as follows: (i) The differences in the transesterification activities of WT and D33N enzymes closely parallel those for the forward reactions with the PI substrate. For example, D33N mutant retained 1.2% activity of the WT enzyme in the transesterification of trifluoroethanol (0.069 and 5.79 μmol min^{-1} mg^{-1}, respectively) as compared to 0.3% activity in the cleavage of PI. (ii) The slopes of the plots of the rates vs pK_a for WT PI-PLC and D33N mutant were -0.10 ± 0.02 and -0.32 ± 0.025, respectively (Figure 6A). The negative slope (increased rate with decreased pK_a) means that alcohol deprotonation is more important than its intrinsic nucleophilicity and implies participation of an enzymic base in the rate-determining step of the transesterification reaction. (iii) The slope of the dependence increases significantly in the mutant, suggesting that alcohol deprotonation becomes more important. (iv) Changes in alcohol pK_a affect the IP/phosphodiester product ratio, such that transesterification becomes a more dominant reaction with more acidic alcohols. Consistently, the steeper slope of the transesterification rate vs pK_a for D33N mutant, as compared to WT PI-PLC, is also reflected in a more pronounced dependence of the transesterification/hydrolysis ratio for the D33N mutant (Figure 6B).

Structural Analysis. The effect of mutations on the protein conformation and conformational stability was examined for all mutants by NMR and Gdn-HCl-induced denaturation, and spectral properties and conformational stability of mutant enzymes were compared with those of WT PI-PLC. Although the primary goal of this work is to examine the catalytic roles of the two Asp−His pairs, it is also important to examine their structural roles for two reasons: (i) The structural characterization is important for the interpretation of the kinetic data and the mutants' structure−function relationships. If the conformation of a mutant is unperturbed, the change in kinetic parameters can be used to explain the functional role of the mutated residue. On the other hand, one cannot attribute the change in kinetic constants solely to the functional role of the mutated residue, if a significant conformational perturbation occurs. (ii) Although Asp···His diads are generally believed to play catalytic functions, we have shown that the Asp-99···His-48 pair at the active site of phospholipase A_2 also plays an important structural role (*38*).

Proton NMR Analyses of the Global Conformation. Both 1D ^{1}H NMR and phase-sensitive NOESY spectra were obtained for the WT and mutant enzymes. As shown by the ^{1}H NMR spectra (Figure 7), His-32 and His-82 mutants and D274A, D274N, and D33N displayed only minor perturbations, since the spectra of H32A, D274A, H82A, and D33A are very similar to that of WT PI-PLC. Although D274E (Figure 7D) has similar features in the aliphatic and aromatic regions, the signals of the amide protons mostly disappeared, indicating that these protons were easily accessible to the solvent. This result suggests that the D274E mutant is more flexible than the WT enzyme.

The enzymes were further analyzed by the NOESY spectra shown in Figure 8. These spectra show little difference between the enzymes in their aromatic−aromatic and aromatic−aliphatic regions. Most of the NOESY cross-peaks observed in WT enzyme are also observable in the H32A, D274A, D274E, H82A, and D33A mutants, and the chemical shifts in the mutants do not significantly differ from those of the WT enzyme. Other mutants including H32N, H32Q, D274N, H82N, H82Q, H82D, and D33N also showed similar 1D- and 2D-NOESY spectra (not shown, but available in Supporting Information) to those of the WT enzyme. These spectra indicated that the global conformations of the mutants are largely preserved, except that of the D274E mutant, which has a more flexible conformation.

Conformational Stability. Comparison of the CD spectra (200−250 nm) for the WT enzyme and all the mutants showed no difference and suggested that the secondary

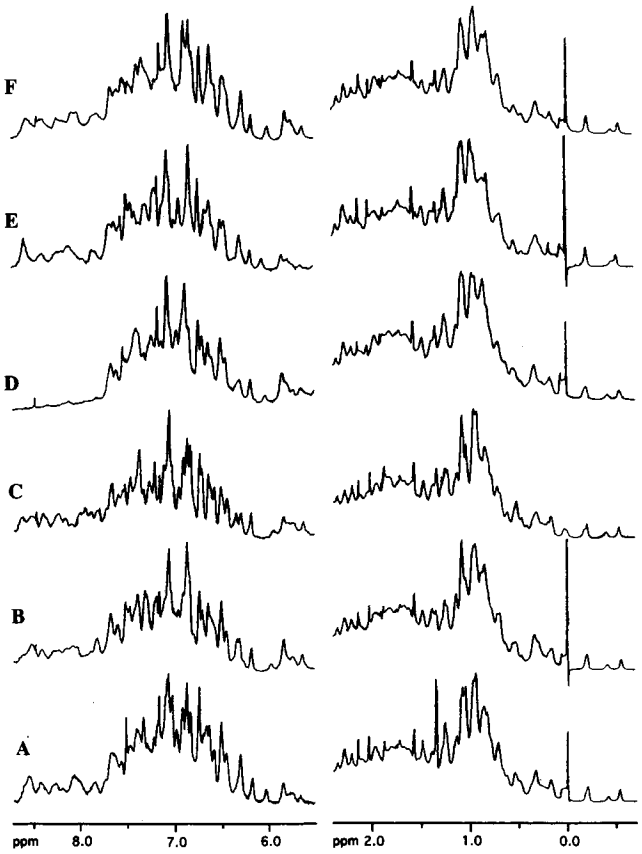

FIGURE 7: One-dimensional proton NMR spectra of WT, H32A, D274A, D274E, H82A, and D33A in D_2O at 600 MHz: (A) WT, (B) H32A, (C) D274A, (D) D274E, (E) H82A, and (F) D33A. Chemical shifts were referenced to internal TMSP-d_4, and the residual water peak was suppressed by 3-9-19 pulse sequence with gradients. Prior to Fourier transformation, the time domain data were zero-filled to 32K points and processed by a Gaussian function (GB = 0.1, LB = −3).

structures are preserved (spectra not shown). The conformational stability of mutants and WT was measured by Gdn-HCl-induced denaturation monitored by CD spectroscopy. The denaturation curves of all mutants and the WT enzyme (data not shown) displayed a behavior consistent with an apparent two-state folding mechanism. The denaturation data were analyzed with the following equation (*31*):

$$\Delta G_d = \Delta G_d^{H_2O} - m[\text{Gdn-HCl}]$$

where ΔG_d is the Gibbs free energy change at various concentration of Gdn-HCl, $\Delta G_d^{H_2O}$ is that at zero concentration of Gdn-HCl, and m is a constant related to the susceptibility of the protein to denaturation. The $\Delta G_d^{H_2O}$ values, the midpoint of the denaturation curve ($D_{1/2}$), and the negative slope (m) are listed in Table 4. Mutation of His-32 (H32A, H32N, H32Q) or His-82 (H82A, H82N, H82Q, and H82D) did not cause any significant change of $\Delta G_d^{H_2O}$. However, all three D274 mutants showed a large decrease (3.9−5.5 kcal/mol) in $\Delta G_d^{H_2O}$. These results suggest that D274 is important in maintaining the conformational stability of PI-PLC, which could contribute to the difficulty encountered during the purification of these mutants. The greater susceptibility of D274E to denaturation is also consistent with the conclusion from NMR studies, indicating that this mutant is conformationally more flexible than the WT enzyme. Overall, the results of NMR and CD analyses indicate that the global conformation and conformational stability are not changed for the mutants studied, with the possible exception of the mutants at position 274.

DISCUSSION

Now that a large body of structure−function data has been obtained for PI-PLC (this paper and refs *18* and *19*), it is appropriate to present the entire view of the catalytic mechanism that we have drawn from this and the previous studies.

Ribonuclease A as a Mechanistic Paradigm for PI-PLC. The development of phosphorothioate analogues allowed study of the reaction mechanism of ribonuclease A (*39, 40*). The stereochemical results demonstrated that both steps of the RNase A reactions, cleavage of UpC and ring opening of 2′,3′-cyclic UMP, occur via an in-line attack, each resulting in the inversion of configuration at the phosphorus center (*39, 40*). The stereochemical mechanism of PI-PLC was elucidated in a similar fashion using phosphorothioate and oxygen isotope labeled analogues (*12, 13*). The results of those studies demonstrated that both bacterial and mammalian PI-PLC catalyze two consecutive steps featuring an in-line nucleophilic attack, resulting in the overall retention of configuration at the phosphorus atom. This finding immediately suggested that PI-PLC uses a mechanism similar to that of RNase A (*12*). This hypothesis was later supported by the crystal structure of PI-PLC from *B. cereus* complexed with *myo*-inositol (*11, 32*) which showed an active site with two histidine residues that could be superimposed on the active site histidines of RNase A.

The analogies between these two enzymes extend, however, well beyond the structures of their active sites: (i) Both enzymes form energetically rich, cyclic five-membered phosphate as their *final* product (*41, 42, 43*). This is due to the 10^3-fold higher rate of transphosphorylation vs hydrolysis for both PI-PLC (*8*) and various RNases (*41, 42*). (ii) Both enzymes require a complete structure of the natural leaving group for their full catalytic efficiency, such as the hydrophobic diacylglycerol moiety (PI-PLC, *8, 44, 45*), or an additional nucleotide at the P2-binding site (*46*). For example, methyl cytidine phosphate, which is a RNase A substrate with a truncated leaving group, is ca. 10^3-fold less reactive than CpA (*42*). Likewise, glycerol inositol phosphate (GroPI), which is an analogue of PI with a truncated leaving group, is 10^3-fold less reactive than PI (K. S. Bruzik and others, unpublished). In summary, the analogies between PI-PLC and RNase A extend into the area of a general strategy that these enzymes use to modulate their activity and to produce energetically rich cyclic phosphates as their final products. It appears that both enzymes use an induced-fit mechanism dependent on binding of the leaving group. The cleavage of the leaving group disconnects the two elements of the substrate required for activity, presumably causing the reversion of the enzyme to its less active conformation.

Structure−Function Study of PI-PLC. Although the crystal structure of bacterial PI-PLC·*myo*-inositol complex has been obtained (*11, 32*) and a number of active site residues have been identified, it is important to perform functional studies to support and refine the enzyme−substrate interactions since *myo*-inositol does not have the diacyl-

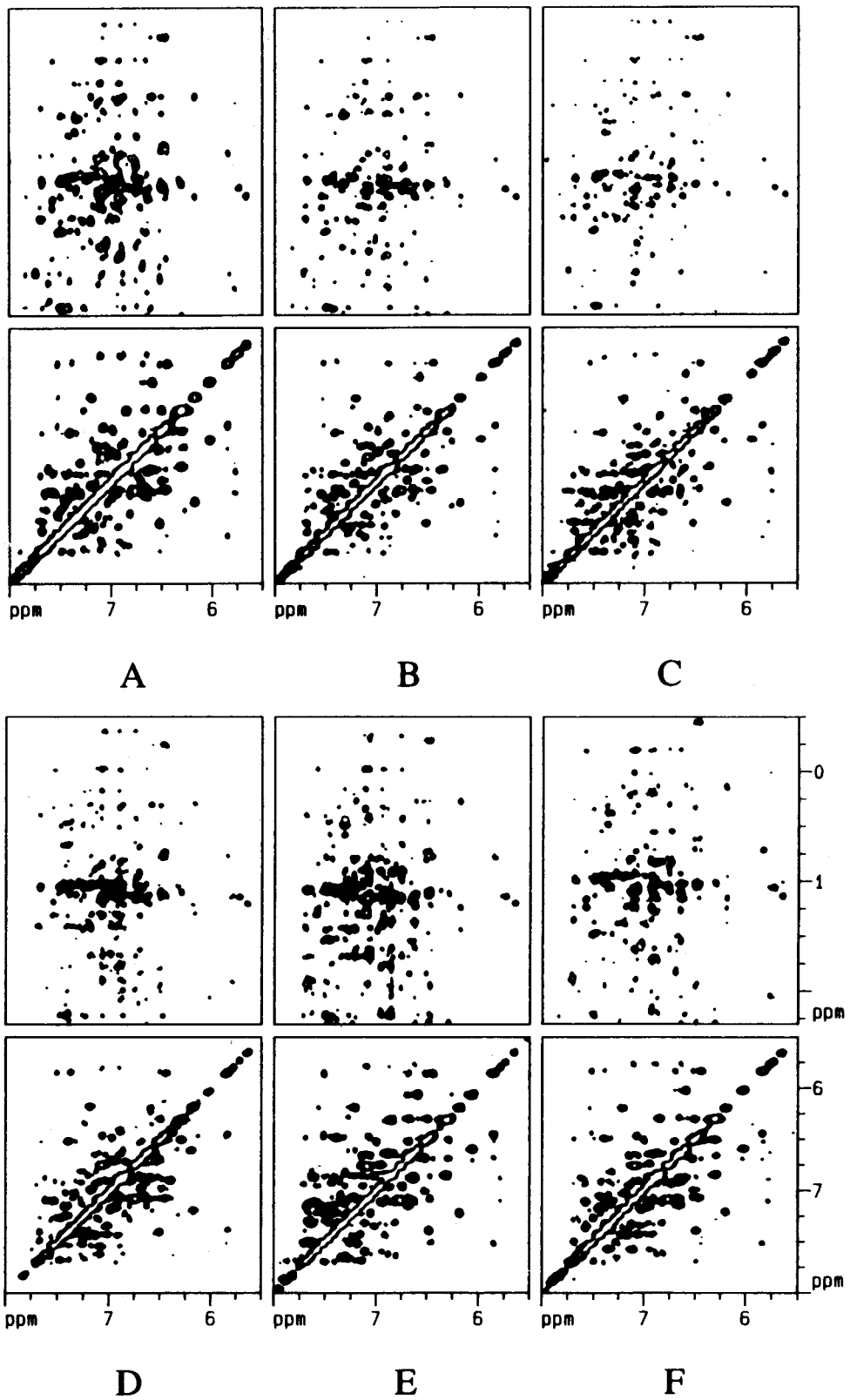

FIGURE 8: Two-dimensional NOESY spectra of WT, H32A, D274A, D274E, H82A, and D33A in D_2O at 600 MHz: (A) WT, (B) H32A, (C) D274A, (D) D274E, (E) H82A, and (F) D33A. The samples contained 0.2 mM enzyme in D_2O at 37 °C at pH 6.8. All spectra were obtained in the phase-sensitive mode with a mixing time of 100 ms. Generally, a 2K × (400−512) time domain matrix was acquired. The two-dimensional data matrix was multiplied by a shifted sine bell function (SSB1 = 8) in t_1 and by a Gaussian function (LB = −3, GB = 0.1) in t_2. The data matrix was then zero-filled to 2K × 1K matrix prior to Fourier transformation.

glycerol moiety and since the enzyme may undergo conformational changes upon substrate binding. It was shown that mutation of either His-32 or His-82 to leucine or alanine resulted in inactive mutants (*11*, *29*, *33*). The catalytic role of these histidines was further confirmed in this work by showing that mutation of either His-32 or His-82 to alanine decreased specific activities by a factor of 10^5. In our earlier work, we have demonstrated that Arg-69 is responsible for

Table 4: Free Energy of Denaturation Induced by Gdn-HCl for Wild-Type PI-PLC and Mutant[a]

enzyme	$\Delta G_d^{H_2O}$ (kcal/mol)	m [kcal/(mol·M)]	$D_{1/2}$ (M)
WT	7.0	3.6	2.0
H32A	7.2	3.9	1.8
H32N	7.1	4.0	1.8
H32Q	6.7	4.4	1.5
H82A	6.0	2.5	2.4
H82N	7.5	3.7	2.0
H82Q	5.0	2.6	1.9
H82D	6.3	3.5	1.8
D274A	2.0	1.8	1.1
D274N	3.1	2.6	1.2
D274E	1.5	0.9	1.6
D33A	7.4	3.6	2.0
D33N	7.5	3.3	2.3

[a] Measured at 19 °C, pH 7.5, 10 mM borate, and 0.1 mM EDTA. The estimated error limit of $\Delta G_d^{H_2O}$ is 0.5 kcal/mol.

the extremely high stereospecificity of the enzyme with regard to configuration at the phosphorus atom in the phosphorothioate analogues and that this most likely occurs due to the interaction between the *pro-S* oxygen of the phosphate group and the Arg-69 residue (*17*, *18*). In addition, the crystal structure indicated that the 3-OH group of inositol made a specific interaction with Asp-198. We have shown prior to structure publication that inversion at the 3-position of inositol causes a 10^3-fold rate decrease (*47*), and we have now demonstrated that D198A mutant cleaves the *chiro*-PI analogue (with inverted 3-OH) with a similar rate to that of PI, further underscoring the interaction of Asp-198 with inositol 3-OH (R. J. Hondal and others, unpublished). In summary, using site-directed mutagenesis in combination with various PI analogues, we have largely confirmed the X-ray model of inositol binding in the active site of PI-PLC.

Description of the Complete Mechanism. On the basis of the results presented in this paper and the previous work from our laboratory and others, we propose that the complete catalytic mechanism of PI-PLC consists of three elements: (i) activation of the inositol 2-hydroxyl group by a general base B_1 to increase its nucleophilicity, (ii) decrease of the negative charge of the phosphate group via hydrogen bonding/protonation by a general acid B_2H to enable approach of the nucleophile to the phosphorus atom, and (iii) electrophilic assistance to the leaving group via protonation/hydrogen bonding of the glycerol O3 oxygen by a general acid B_3H. As will be discussed below, each of the three elements contributes an acceleration factor of ca. 10^5. The analogous three elements are present in the catalytic mechanism of ribonuclease A.

Asp-274 and His-32 Function Together as a "Catalytic Diad". As discussed above, the results of our mutagenesis studies largely support the orientation of *myo*-inositol in the active site of *B. thuringiensis* PI-PLC shown by the crystal structure. On the basis of the structural data, His-32 is the only residue close enough to deprotonate the 2-OH group of inositol to initiate the nucleophilic attack. Mutation of His-32 to alanine results in a 10^5-fold rate reduction, confirming the important role of His-32 in catalysis. The equivalent base in RNase A (His-12) also contributes a factor of 10^4 toward catalysis (*48*). It is obvious that Asp-274 also plays an important catalytic role. The D274A mutation causes a decrease in the catalytic efficiency by a factor of 10^4, thus indicating that Asp-274 is only slightly less important than His-32. We believe that the role of Asp-274 is to enhance the basicity of His-32 or to orient His-32 in the correct position and tautomeric form for catalysis. This function would be similar to that of the catalytic diad of phospholipase A_2 (*20*) and the catalytic triad of serine proteases (*21*). The relatively high activity of D274N mutant (ca. 2% of WT) can be explained by the fact that asparagine is isosteric with aspartate and should still be able to form hydrogen bonds with His-32, thus orienting it correctly for catalysis. Asp-274 probably plays a structural role as well, since mutations at this position result in enzymes with greatly decreased stability toward Gdn-HCl-induced denaturation.

Arg-69 Interacts with the Phosphate Group via Hydrogen Bonding or Protonation to a Nonbridging Oxygen. We have previously demonstrated that mutation of Arg-69 to alanine results in a loss of activity by a factor of 5×10^4 (*17*). The functional role of this residue was unambiguously assigned by studying the kinetic behavior of WT and mutant PI-PLC with phosphorothioate analogues of PI. We have shown that the WT enzyme favors the R_p-phosphorothioate over the S_p-isomer by a factor of 10^5 (*17*) and that this extremely high stereoselection is due to a low rate of cleavage of the S_p-isomer, whereas the rate of cleavage of the R_p-isomer is only slightly lower than that of PI. We have also demonstrated that mutation of Arg-69 to lysine results in the 10^4-fold reduction in stereoselectivity (*17*). Such a large change in the stereoselectivity toward phosphorothioate isomers upon mutation is strong evidence that the side chain of Arg-69 interacts directly with the phosphate moiety of phosphatidylinositol. We believe that the mechanism that accounts for such a large stereoselectivity involves hydrogen bonding/protonation of the *pro-S* oxygen by Arg-69 in the transition state, although the extent of proton transfer between Arg-69 and the oxygen atom of the transition state remains an open question. A similar functional role was assigned recently to Lys-41 of RNase A (*49*). The function of this hydrogen bond is to "activate" the phosphodiester toward nucleophilic attack and help orient the phosphate group in the correct position for catalysis. The replacement of the *pro-S* oxygen by sulfur results most likely in a loss of the hydrogen bond and a great impairment of the catalytic efficiency. This conclusion is supported by the fact that no hydrogen bond to a sulfur atom has been found in any of the available nucleoside phosphorothioate crystal structures (*50*). The proposed function of Arg-69 is also consistent with the modeled structure of PI-PLC complex with methyl inositol 1,2-cyclic oxyphosphorane showing that the guanidinium side chain of Arg-69 is within the required distance for proton transfer (2.8 Å) (K. S. Bruzik and P.-G. Nyholm, unpublished results).

His-82 Functions as a General Acid with Assistance from Asp-33. Both His-82 and Asp-33 mutants displayed significantly lower catalytic efficiencies toward PI substrate, indicating important catalytic roles of these residues. Further details of the function of His-82 and Asp-33 were obtained in this and the previous work (*18*) based on the observation that mutation at these positions affects the catalytic efficiency to a much smaller extent, if the substrate features a thiol or a *p*-nitrophenol as a leaving group. Thus, mutation of His-82 to alanine results in a 10^5-fold decrease of the activity toward the natural PI, but only a 500-fold decrease with the

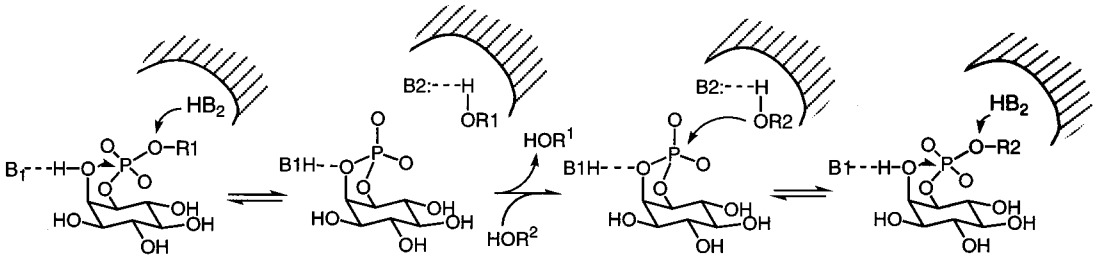

FIGURE 9: Mechanism of PI-PLC-catalyzed transesterification of short-chain alcohols with IcP showing alcohol exchange in the ternary complex.

phosphorothiolate analogue of PI, DPsPI, and a 16-fold reduction with NPIPs. Likewise, the mutation of Asp-33 to alanine causes a 10^3-fold drop in activity toward PI but only a 4-fold decrease with DPsPI (*18*) and a 3-fold reduction with NPIPs**.** As a result, these mutants cleave DPsPI 10-fold faster than the natural PI substrate, displaying what we have termed a reverse thio-effect (*18*). Similarly, NPIPs is cleaved more quickly by these mutants than the PI substrate (60-fold faster by H82A, and 30-fold faster by D33A mutant). This effect is almost certainly related to the lower pK_a's of the leaving groups of the thiol analogue of diacylglycerol and *p*-nitrophenol as compared to the hydroxyl leaving group of diacylglycerol. Due to the paucity of the pK_a data for the above leaving groups, one can use instead the pK_a values of their nonacylated parent compounds for comparison of the properties of these leaving group. The parent compound for PI, glycerol, has a pK_a of 14.2 (*51*); the parent compound for DPsPI, thioglycerol, has a pK_a of 9.51 (*52*); and the pK_a of *p*-nitrophenol is 7.14. The observed rates of the phosphorothiolate cleavage are the result of two partially compensating effects: (i) the presence of sulfur on the leaving group reduces stabilization of the transition state by the general acid (presumably a 10^5-fold effect) due to a loss of hydrogen bonding to the leaving group; but (ii) the lower pK_a of the thiol group allows more negative charge to be developed on the sulfur atom and, hence, stabilizes the transition state. A related effect has been observed for RNase A, where activity was reduced 10^5-fold upon mutation of His-119 to alanine but was restored to the wild-type level with uridine 3′-*p*-nitrophenyl phosphate as a substrate (*48*). This effect was attributed to the low pK_a of the *p*-nitrophenol leaving group.

The results with H82A and D33A mutants and the PI analogues clearly implicate both of these residues in the role of the general acid assisting the departure of the leaving group. We believe that His-82 is acting as a general acid in a direct manner, while Asp-33 is involved in a supporting role. This conclusion is consistent with the decrease of the pK_a of His-82 from 7.0 to 6.2 upon D33N mutation. The effect of this mutation can be explained, if it is assumed that Asp-33 stabilizes the positive charge of the imidazolium group of His-82; the change of Asp-33 to Asn should weaken this stabilization and lower the pK_a of His-82.

Effect of D33N Mutation on Transesterification. If the entire cleavage reaction is a single-step process, then the effect of mutations on the reverse reaction, such as transesterification of short-chain alcohols with IcP, should be analogous to those observed for the forward reaction. This conclusion is consistent with effects of mutations on the rate of IcP hydrolysis, where most mutants studied showed decreases of activity analogous to those observed in the PI cleavage. In the reverse reaction, the protonation status of the general acid−general base (GA−GB) couple should be reversed, i.e., the GA of the forward reaction should become the GB in the reverse (transesterification) reaction, to effect deprotonation of the incoming external alcohol. The degree of alcohol deprotonation in the reverse reaction (which should be the same as the degree of protonation in the forward reaction) should depend on the alcohol pK_a and the strength of the enzymic base. The externally added alcohol undergoes an exchange with an alcohol of a ternary complex of the products **(**Figure 9) and uses the binding site formerly occupied by the leaving group alkoxide (*10*). The WT PI-PLC showed a small Brønsted coefficient of $\beta_{nuc} = -0.10 \pm 0.02$, somewhat lower than that obtained for reactions of RNase A with phenyl esters of uridine 3′-phosphate (-0.17 ± 0.03; *53*). The rate of the transesterification reaction increased with the decrease of pK_a, indicating that alcohol deprotonation, not an intrinsic nucleophilicity of nonionized alcohol, is the predominant factor. The low absolute value of β_{nuc} (small slope) for the WT PI-PLC can be rationalized in two ways: (i) The rate of the reaction of an alcohol with IcP is the function of both intrinsic nucleophilicity of alcohol and the degree of its ionization. These two effects are compensatory in nature, and the small negative value of β_{nuc} could mean that deprotonation of alcohol predominates slightly. (ii) The transition state involves only a small degree of charge development on the attacking alcohol oxygen (in the forward reaction it would mean a high degree of leaving group protonation). For comparison, the nonenzymatic, imidazole-catalyzed cleavage of ribonucleotides is associated with β_{nuc} values greater that -0.5 (*54*), indicating a large degree of negative charge development on the leaving group. The 3-fold higher β_{nuc} coefficient (-0.32 ± 0.025) obtained for the D33N mutant, as compared to WT PI-PLC, can be explained by a lower ability of its His-82 to donate a proton to the leaving group in the forward reaction. Hence, in the transition state for the reaction of this mutant more negative charge is developed on the leaving group at the cost of the higher energy of the transition state. In summary, the above results clearly point to Asp-33 as a part of the composite general acid function (Asp-33···His-82).

Conclusions. Overall, the present study has enhanced our understanding of the functional roles of enzymic residues beyond that proposed on the basis of the crystal structure of Heinz et al. (*11*). The results obtained are in agreement with the classical general base−general acid mechanism, reminiscent of that of RNase A. In addition, the arginine−phosphate interaction also plays an important role. The detailed mechanism inferred form the results reported in this and our previous papers is described in Figure 10. According to such a mechanism, the general base His-32 abstracts the

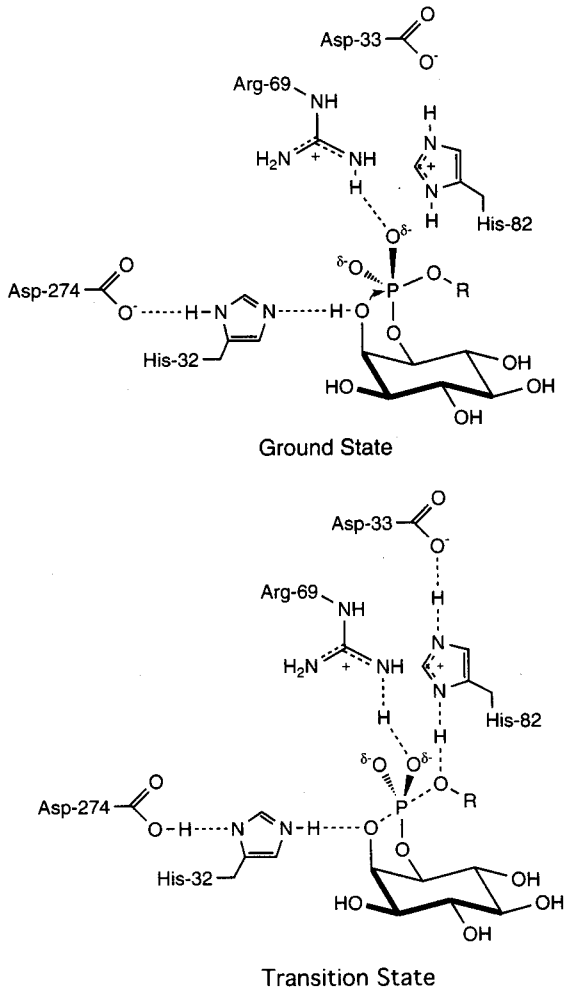

FIGURE 10: Function of catalytic residues of *B. thuringiensis* PI-PLC in the ground and transition states deduced from this study.

proton from the 2-OH of inositol. The general base function of His-32 is enhanced by Asp-274. This occurs with the concomitant activation of the phosphodiester by a hydrogen bond between Arg-69 and the *pro-S* oxygen of the phosphate group. As the attacking nucleophile moves toward the phosphorus atom, the hydrogen bond strengthens and proton transfer to the nonbridging oxygen may occur. The departure of the O3 oxygen of the diacylglycerol leaving group is facilitated by proton donation from the imidazolium form of His-82. The general acid form of this residue is enhanced by Asp-33. The low Brønsted coefficient suggests a significant degree of leaving group protonation. In the second reaction, hydrolysis of IcP, the roles of the two histidines are reversed. His-82 abstracts a proton from a water molecule, which then attacks the phosphorus center. An analogous trigonal bipyramidal transition state is formed in the hydrolysis of IcP as in the conversion of PI to IcP. The protonated form of His-32 now acts as a general acid to donate a proton to the 2-OH group of inositol, thus completing the catalytic cycle. The results presented in this work have enhanced our understanding of the catalytic mechanisms of both PI-PLC and RNase A.

ACKNOWLEDGMENT

We thank Dr. Qunhui Li for constructing H82N and H82Q mutants and Ashlie Burkart and Xiaokui Mo for purifying H82N and H82Q mutants.

SUPPORTING INFORMATION AVAILABLE

One-dimensional proton NMR spectra of WT, H32N, H32Q, D274N, H82N, H82Q, H82D, D33N, and WT PI-PLC (Figure 1); 2D NMR NOESY spectra of WT, H32N, H32Q, D274N, and WT PI-PLC (Figure 2); and 2D NMR NOESY spectra of H82N, H82Q, H82D, and D33N (Figure 3) (3 pages). Ordering information is given on any current masthead page.

REFERENCES

1. Rhee, S. G., Suh, P.-G., Ryu, S. H., & Lee, S. Y. (1989) *Science 244*, 546−550.
2. Turner, A. J. (1990) *Molecular and Cell Biology of Membrane Proteins, Glycolipid Anchors of Cell-Surface Proteins*, pp 5−220, Ellis Horwood, Chichester, U.K.
3. Dennis, E. A., Rhee, S. G., Billah, M. M., and Hannun, Y. A. (1991) *FASEB J. 5*, 2068−2077.
4. Bruzik, K. S., and Tsai, M.-D. (1994) *Bioorg. Med. Chem. 2*, 49−72.
5. Dekker, L. V., Palmer, R. H., and Parker, P. J. (1995) *Curr. Opin. Struct. Biol. 5*, 396−402.
6. Berridge, M. J. (1993) *Nature 361*, 315−325.
7. Low, M. G., and Saltiel, A. R. (1988) *Science 239*, 268−275.
8. Volwerk, J. J., Shashidhar, M. S., Kuppe, A., and Griffith, O. H. (1990) *Biochemistry 29*, 8056−8062.
9. Zhou, C., Wu, Y., and Roberts, M. F. (1997) *Biochemistry 36*, 347−355.
10. Bruzik, K. S., Guan, Z., Riddle, S., and Tsai. M.-D. (1996) *J. Am. Chem. Soc. 118*, 7679−7688.
11. Heinz, D. W., Ryan, M., Bullock, T. L., and Griffith, O. H. (1995) *EMBO J. 14*, 3855−3863.
12. Bruzik, K. S., Morocho, A. M., Jhon, D.-Y., Rhee, S. G., and Tsai, M.-D. (1992) *Biochemistry 31*, 5183−5193.
13. Lin, G., Bennett, F., and Tsai, M.-D. (1990) *Biochemistry 29*, 2747−2757.
14. Essen, L.-O., Perisic, O., Cheung, R., Katan, M., and Williams, R. L. (1996) *Nature 380*, 595−602.
15. Essen, L.-O., Perisic, O., Katan, M., Wu, Y., Roberts, M. F., and Williams, R. L. (1997) *Biochemistry 36*, 1704−1718.
16. Kuppe, A., Evans, L. M., McMillen, D. A., and Griffith, O. H. (1989) *J. Bacteriol. 171*, 6077−6083.
17. Hondal, R. J., Riddle, R. R., Kravchuk, A. V., Zhao, Z., Bruzik, K. S., and Tsai, M.-D. (1997) *Biochemistry 36*, 6633−6642.
18. Hondal, R. J., Bruzik, K. S., Zhao, Z., and Tsai, M.-D. (1997) *J. Am. Chem. Soc. 119*, 5477−5478.
19. Hondal, R. J., Bruzik, K. S., and Tsai, M.-D. (1997) *J. Am. Chem. Soc. 119*, 9933−9934.
20. Sekar, K., Yu, B. Z., Rogers, J., Lutton, J., Liu, X., Chen, X., Tsai, M.-D., Jain, M. K., and Sundaralingam, M. (1997) *Biochemistry 36*, 3104−3114.
21. Craik, C. S., Roczniak, S., Largman, C., and Rutter, W. J. (1987) *Science 237*, 909−913.
22. Daugherty, S., and Low, M. G. (1993) *Infect. Immun. 61*, 5078−5089.
23. Mihai, C., Mataka, J., Riddle, S., Tsai, M.-D., and Bruzik, K. S. (1997) *Bioorg. Med. Chem. Lett. 7*, 1235−1238.
24. Kunkel, T. A. (1985) *Proc. Natl. Acad. Sci. U.S.A. 82*, 488−492.
25. Griffith, O. H., Volwerk, J. J., and Kuppe, A. (1991) *Methods Enzymol. 197*, 493−502.
26. Hendrickson, H. S., Hendrickson, E. K., Johnson, J. L., Khan, T. H., and Chial, H. J. (1992) *Biochemistry 31*, 12169−12172.
27. Bax, A., Ikura, M., Kay, L. E., Torchia, D. E., and Tschudin, R. (1990) *J. Magn. Reson. 86*, 304−318.
28. Kay, L. E., Keifer, P., and Saarinen, T. (1992) *J. Am. Chem. Soc. 114*, 10663−10665.
29. Liu, T., Ryan, M., Dahlquist, F. W., and Griffith, O. H. (1997) *Protein Sci. 6*, 1−8.
30. Nozaki, Y. (1972) *Methods Enzymol. 26*, 43−50.
31. Pace, C. N. (1986) *Methods Enzymol. 131*, 266−280.

32. Heinz, D. W., Ryan, M., Smith, M. P., Weaver, L. H., Keana, J. F. W., and Griffith, O. H. (1996) *Biochemistry 35*, 9496−9504.
33. Gässler, C. S., Ryan, M., Liu, T., Griffith, O. H., and Heinz, D. W. (1997) *Biochemistry 36*, 12802−12813.
34. Yu, L., and Dennis, A. A. (1991) *Methods Enzymol. 197*, 65−75.
35. Herschlag, D., Piccirilli, J. A., and Cech, T. R. (1991) *Biochemistry 30*, 4844−4854.
36. Piccirilli, J. A., Vyle, J. S., Caruthers, M. H., and Cech, T. R. (1993) *Nature 361*, 85−88.
37. Leigh, A. J., Volwerk, J. J., Griffith, O. H., and Keana, J. F. W. (1992) *Biochemistry 31*, 8978−8983.
38. Li, Y., and Tsai, M.-D. (1993) *J. Am. Chem. Soc. 115*, 8523−8526.
39. Usher, D. A., Richardson, D. I., Jr., and Eckstein, F. (1970) *Nature 228*, 663−668.
40. Usher, D. A., Erenrich, E. S., and Eckstein, F. (1972) *Proc. Natl. Acad. Sci. U.S.A. 69*, 115−121.
41. Cuchillo, C. M., Pares, X., Guasch, A., Barman, T., Travers, F., and Nogues, M. V. (1993) *FEBS Lett. 3*, 207−210.
42. Thompson, J. E., Venegas, F. D., and Raines, R. T. (1994) *Biochemistry 33*, 7408−7414.
43. Sorrentino, S., and Libonati, M. (1997) *FEBS Lett. 404*, 1−5.
44. Lewis, K. A., Garigapati, V. R., Zhou, C., and Roberts, M. F. (1993) *Biochemistry 32*, 8836−8841.
45. Rebecchi, M. J., Eberhardt, R., Delaney, T., Ali, S., and Bittman, R. (1993) *J. Biol. Chem. 268*, 1735−1741.
46. Boix, E., Nogues, M. V., Schein, C. H., Benner, S. A., and Cuchillo, C. M. (1994) *J. Biol. Chem. 269*, 2529−2534.
47. Bruzik, K. S., Hakeem, A. A., and Tsai, M.-D. (1994) *Biochemistry 33*, 8367−8374.
48. Thompson, J. E., and Raines, R. T. (1994) *J. Am. Chem. Soc. 116*, 5467−5468.
49. Messmore, J. M., Fuchs, D. N., and Raines, R. T. (1995) *J. Am. Chem. Soc. 117*, 8057−8060.
50. Hinrichs, W., Steifa, M., Saenger, W., and Eckstein, F. (1987) *Nucleic Acids Res. 15*, 4945−4955.
51. Weast, R. C., and Astle, M. J. (1980) in *CRC Handbook of Chemistry and Physics* (Weast, R. C., and Astle, M. J., Eds.) pp D164−D168, CRC Press, Boca Raton.
52. Danehy, J. P., and Parameswaran, K. N. (1968) *J. Chem. Eng. Data 13*, 386−389.
53. Davis, A. M., Regan, A. C., and Williams, A. (1988a) *Biochemistry 27*, 9042−9047.
54. Davis, A. M., Hall, A. D., and Williams, A. (1988b) *J. Am. Chem. Soc. 110*, 5105.

BI972646I